

Research

Identification and Functional Analysis of Git3 G Protein-Coupled Receptors in *Ganoderma boninense* PER71

Khairunnisa Hanisah Mohd Daud¹, Mohd Faizal Abu Bakar², Izwan Bharudin¹, Shazilah Kamaruddin¹, Doris Huai Xia Quay³, Farah Diba Abu Bakar¹, Abdul Munir Abdul Murad^{1*}

1. Department of Biological Sciences and Biotechnology, Faculty of Science and Technology, Universiti Kebangsaan Malaysia, 43600 UKM Bangi, Selangor, Malaysia
2. Malaysia Genome and Vaccine Institute, National Institute of Biotechnology Malaysia (NIBM), Jalan Bangi, 43000 Kajang, Selangor, Malaysia
3. Department of Applied Physics, Faculty of Science and Technology, Universiti Kebangsaan Malaysia, 43600 UKM Bangi, Selangor, Malaysia

*Corresponding author: munir@ukm.edu.my

ABSTRACT

G protein-coupled receptors (GPCRs) are integral components of eukaryotic heterotrimeric G proteins, playing crucial roles in detecting extracellular signals and initiating the activity of signaling proteins within cells to activate cellular responses to these signals. The objectives of this study are to identify and characterize the function of Git3, a Class III GPCR protein, in the oil palm pathogen *Ganoderma boninense*. To identify the potential genes encoded for GPCR in this fungus, intensive data mining on the genome and transcriptome data has been carried out. A total of six classes of GPCRs have been identified. These include Class II pheromone detectors, Class III carbon detectors, Class IV nitrogen detectors, Class VII proteins similar to glycosyltransferase, Class VIII proteins similar to hemolysin, and Class X protein receptors. Among these, the Class III protein Git3, postulated to be involved in glucose sensing and fungal pathogenicity, was selected for gene knockdown using RNA interference (RNAi). A plasmid, designated pUChph-GIT3, was constructed, to target *git3* silencing by incorporating a hygromycin resistance gene cassette and antisense sequences of *git3*. Transformation of *G. boninense* PER71 with pUChph-GIT3 produced five potential $\Delta git3$ gene-silenced mutants. PCR analysis confirmed the integration of the RNAi expression cassette into the fungal genome. Quantitative PCR (qPCR) analysis revealed significant reductions in *git3* expression in three *G. boninense* mutants, M42, M66, and M5 by 47%, 23%, and 13%, respectively. The Disease Severity Index (DSI) indicated slower disease progression in oil palm plantlets infected with $\Delta git3$ mutants compared to those infected with wild-type *G. boninense* PER71. In conclusion, this study successfully isolated and characterized the *git3* GPCR from *G. boninense* and demonstrated that it might play a role during the early stages of infection, as the mutants were able to slow the progression of infection in oil palm plantlets.

Key words: Artificial infection, carbon sensor, G Protein-Coupled receptors, Git3, RNA interference, short hairpin RNA

Article History

Accepted: 26 August 2024

First version online: 27 October 2024

Cite This Article:

Mohd Daud, K.H., Bakar, M.F.A., Bharudin, I., Kamarudin, S., Quay, D.H.X., Bakar, F.D.A. & Murad, A.M.A. 2024. Identification and functional analysis of GIT3 G protein-coupled receptors in *Ganoderma boninense* PER71. Malaysian Applied Biology, 53(4): 125-137. <https://doi.org/10.55230/mabjournal.v53i4.3126>

Copyright

© 2024 Malaysian Society of Applied Biology

INTRODUCTION

Ganoderma orbiforme is a white-rot fungus responsible for causing Basal Stem Rot (BSR) (Azmi *et al.*, 2020) and Upper Stem Rot (USR) (Nur-Rashyeda *et al.*, 2023) diseases in oil palms. These diseases can reduce up to 80% of the productivity of infected oil palms (Paterson, 2019), leading to significant economic losses for major oil palm producers and exporters like Indonesia and Malaysia. These losses can collectively amount to as much as RM1.5 billion annually (Khaled *et al.*, 2020).

Current strategies to combat BSR include sanitation practices, surgical interventions, the application of chemical antifungal compounds, and the use of biocontrol agents (Khairi *et al.*, 2022). However, these methods have proven insufficient, as they cannot completely eradicate BSR at all infected sites and are most effective when the disease is detected in its early stages. The varied effectiveness of

these strategies can be attributed to the complex behavior of *G. boninense*, which exhibits tolerance to these treatments. This tolerance may be linked to the high genetic variation within *G. boninense*, resulting from its tetrapolar mating system (Bharudin *et al.*, 2022). Additionally, the spread of the disease through wind-borne basidiospores and vectors poses a significant challenge to maintaining the efficacy of control strategies. Consequently, ongoing research is focused on developing new approaches to effectively reduce the incidence of BSR and control its spread. The availability of several genome and transcriptome datasets for *G. boninense* has significantly enhanced the understanding of the fundamental biology of this fungus (Mercière *et al.*, 2015; Isaac *et al.*, 2018; Utomo *et al.*, 2018; Sulaiman *et al.*, 2020; Khairi *et al.*, 2022).

The identification of G protein-coupled receptors (GPCRs) in fungi may hold the key to addressing basal stem rot (BSR) disease, as GPCRs play crucial roles in signaling pathways in all eukaryotes. GPCRs are part of the seven transmembrane domains in heterotrimeric G proteins, which are involved in signal transduction pathways found in every eukaryote. Heterotrimeric G proteins consist of three subunits that form trimers: alpha ($G\alpha$), beta ($G\beta$), and gamma ($G\gamma$) (Wess *et al.*, 2008). The external receptor identifies and binds to the GPCR ligand, triggering the exchange of GDP for GTP in the $G\alpha$ subunit. This causes the separation of the $G\alpha$ subunit from the $G\beta\gamma$ complex, leading to changes in other secondary metabolites that initiate downstream signaling pathways. In ascomycete fungi, $G\alpha$ is involved in activating the cAMP-PKA pathway (Kraakman *et al.*, 1999) while in basidiomycete fungi, $G\beta\gamma$ is involved in mating (Raudaskoski & Kothe, 2010). G proteins are also essential for various cellular processes in fungi, including mating, virulence establishment, pathogenic development, cell division, morphogenesis, chemotaxis, and the synthesis of secondary metabolites. GPCRs have been identified in several fungi, including *Saccharomyces cerevisiae*, *Candida albicans*, *Aspergillus nidulans*, *Aspergillus fumigatus*, *Aspergillus oryzae*, *Magnaporthe grisea*, *Cryptococcus neoformans*, *Neurospora crassa*, *Verticillium* spp. and *Trichoderma* spp. (Lafon *et al.*, 2006).

In the model fungal ascomycete *Aspergillus nidulans*, ten classes of G protein-coupled receptors (GPCRs) have been identified, including Class I and Class II pheromone sensors, Class III carbon sensors, Class IV nitrogen sensors, Class V secretin-like receptors, Class VI RGS domain-containing receptors, Class VII MG00532-like receptors, Class VIII hemolysin-related receptors, Class IX opsins, and Class X PTH11-like receptors. However, only a few of these classes have been functionally studied (Brown *et al.*, 2018). Numerous investigations have demonstrated a strong correlation between fungal reproduction and the production of secondary metabolites, which is mediated by GPCR sensing of signaling molecules, particularly pheromones, nutrients, and oxylipins (Gao *et al.*, 2021). Class III fungal GPCRs, which are involved in carbon source sensing, show high similarity to the *S. cerevisiae* Gpr1 receptor (El-Defrawy & Hesham, 2020). In *S. cerevisiae*, Gpr1 functions as a glucose and sucrose sensor (Rubio-Teixeira *et al.*, 2010). The interaction between the GPCR protein Gpr1 and the $G\alpha$ protein Gpa2 is essential for the stimulation of cAMP synthesis by these sugars. In *Aspergillus*, the class III GPCRs GprC and GprD, which are analogous to Gpr1 in *S. cerevisiae*, are involved in the sensing of sugars (Gehrke *et al.*, 2010). Deletion of the *gprC* or *gprD* genes in *A. flavus* also leads to changes in quorum sensing (QS), sporulation, sclerotia formation, and aflatoxin (AF) biosynthesis (Affeldt *et al.*, 2012). In the human pathogen *A. fumigatus*, deleting the *gprC* and *gprD* genes affects the ability of the strains to produce various toxic secondary metabolites, as well as impacts fungal growth and pathogenicity during infections (Gehrke *et al.*, 2010).

Root exudates play a crucial role in determining the chemotactic movement of fungi towards target plants. For pathogenic fungi such as *G. boninense*, root exudates may significantly influence the movement of the fungus towards oil palm roots, leading to infection. Root exudates are rich in carbon sources and require signal receptors on the fungal cell surface to enable a response to these stimuli. Given that Class III GPCRs are sugar sensors, it is likely that they may be involved in detecting the carbon sources present in the oil palm root exudates, which is essential for the pathogenic response of *G. boninense*. Hence, the identification and characterization of Class III GPCRs in *G. boninense* may provide new insights into the pathogenic mechanisms of this fungus, potentially leading to novel strategies for managing basal stem rot (BSR) disease in oil palm.

MATERIALS AND METHODS

Growth media for *G. boninense*

Ganoderma boninense strain PER71 obtained from the Malaysian Palm Oil Board (MPOB) was used in this study. *G. boninense* was grown on CYMA plates (2% glucose, 0.2% g/L peptone, 0.1% yeast extract, 0.05% $MgSO_4$, 0.046% KH_2PO_4 , 0.1% K_2HPO_4 , & 2.0% bacteriological agar) by inoculating and incubating mycelial agar plugs at 28°C for 6 days. The CYMB medium, which contains the same

components as CYMA but without bacteriological agar, was used to grow *G. boninense* mutants for DNA extraction, RNA extraction, and qPCR analysis. *G. boninense* was subcultured every two months for storage.

Genome mining for the GPCR genes in *G. boninense*

To search for the Indigenous genes encoding GPCR, the *G. boninense* PER71 transcriptome database (<https://www.ncbi.nlm.nih.gov/bioproject/PRJNA269646>) (Isaac *et al.*, 2018), *G. boninense* NJ3 genome database (https://www.ncbi.nlm.nih.gov/datasets/genome/GCA_001855635.1/) and *G. boninense* G3 genome database were used (<https://www.ncbi.nlm.nih.gov/bioproject/773636>). *Aspergillus niger* GPCRs are used as the reference genes in BLASTX analysis against all *G. boninense* genome and transcriptome databases. TMHMM (<https://dtu.biolib.com/DeepTMHMM>) (Sonnhammer *et al.*, 1998), Phobius (<https://phobius.sbc.su.se/>) (Käll *et al.*, 2007), and TMPred (<https://bio.tools/TMPred>) (Hofmann & Stoffel, 1993) software are used to analyze the transmembrane protein in GPCRs found in genomic and transcriptomic data mining of *G. boninense*. The phylogenetic tree was generated using MEGA X to compare Class III GPCRs in *G. boninense* PER71 with those of other species, employing the Maximum Likelihood method with 1000 bootstrap replicates (Tamura *et al.*, 2021).

Gene cloning, sequence, and analysis

Oligonucleotide primers designed for the PCR amplification of the *git3* gene based on the reference sequence data of *G. boninense* PER71 are provided in Table 1. The primers were synthesized by Integrated DNA Technologies, Singapore. Genomic DNA extraction of *G. boninense* PER71 was done using modified cetyltrimethylammonium bromide buffer (CTAB) (2% CTAB, 100 mM Tris-HCl pH 8.4, 1.4 M NaCl, 25 mM EDTA), followed by separation using chloroform (Madihah *et al.*, 2018). The PCR amplification of the *git3* gene was carried out using Phanta Max Super Fidelity Polymerase (Vazyme, China). The amplified products were cloned into the pGEM-T Easy vectors (Promega, USA) and the resulting recombinant plasmids were propagated via transformation of *Escherichia coli* TOP10 (Thermo Scientific, USA) cells. Extraction of the plasmids was performed using the Wizard®Plus Minipreps DNA Purification System (Promega, USA). The sequencing of DNA was outsourced to Apical Scientific Sdn. Bhd., Malaysia. The sequencing results of the targeted genes carried by the pGEM-T vectors were then aligned using T-COFFEE M software (<https://tcoffee.crg.eu/>) (Notredame *et al.*, 2000).

Construction of the RNAi cassette

To develop a vector containing siRNA expression cassettes, 1.5 kb of *gpdA* promoter sequence from *A. nidulans* with 300 bp of *git3* terminator sequence containing restriction enzymes *NarI*, *NotI*, *PacI*, and *NheI* was synthesized by Azenta Life Science (China). Similarly, a construct with the size of 591 bp of *git3* that includes the sense and spacer sequences containing enzymes *NotI* and *PacI* and 596 bp of antisense *git3* sequence containing enzymes *PacI* and *NheI* was synthesized by Azenta Life Science (China), and cloned into pUC57. Subsequently, the cassette was assembled into a pUChph vector containing a hygromycin-resistant gene derived from pN1389 and pUC19 as the backbone. pUChph was digested with the enzyme *NarI* and ligated with the promoter-terminator sequence. The confirmed pUChph_promoter-terminator vector then was ligated with sense-spacer and antisense sequences at *NotI-PacI* and *PacI-NheI* restriction sites, respectively, forming the pUChph-*GIT3* shRNAi expression plasmid construct. The pUChph containing the whole siRNA expression cassette with a size of 7852 kb was used to transform *E. coli* TOP10 for plasmid propagation. The resulting plasmids were subsequently validated via restriction enzyme analyses using the enzymes *NarI*, *NotI-NheI*, *NotI-PacI*, and *PacI-NheI*.

Generation of *G. boninense* protoplasts

A total of 60 agar plugs, each with a diameter of 0.8 cm and containing 6-day-old mycelia, were inoculated into a 1 L flask containing 400 mL of CYMB medium. The mixture was incubated for 5 days at 28°C and 250 rpm to promote mycelial proliferation. Next, the mycelia were filtered through sterile Miracloth and rinsed with 0.6 M mannitol to remove any residual growth media before being allowed to drain. The generation of protoplasts was carried out using a modified protocol based on Ab Wahab *et al.* (2022). Approximately 0.3 g of mycelia was placed into a sterile 250 mL conical flask containing 25 mL of osmotic medium (0.6 M mannitol, 10 mM phosphate buffer, pH 5.8) along with 1% lysing enzyme (Sigma-Aldrich, USA). The mixture was incubated at 30°C while shaking at 110 rpm for 2 hr. Following incubation, the protoplasts were purified by filtering the mixture through Miracloth layered with Kimwipes, a process conducted on ice to prevent damage to the protoplasts. The resulting solution containing protoplasts was then centrifuged at 4°C at 1575 × g for 30 min to pellet the protoplasts, after which the supernatant was carefully discarded to avoid disturbing the pellet. The pelleted protoplasts

were resuspended in 2 mL STC solution (0.55 M sorbitol, 10 mM CaCl₂, 10 mM Tris-HCl pH 7.5) and the resuspension step was done slowly to reduce the mechanical pressure which can cause the protoplasts to break. Next, the samples were centrifuged at 4°C, 1575 ×g for 8 min. This step was repeated twice to eliminate any leftover osmotic solution containing lytic enzyme. Finally, the purified protoplasts were resuspended in 200 µL of STC solution and the number of protoplasts produced was counted using a hemocytometer.

PEG-mediated transformation of the *G. boninense* PER71 protoplasts with pUChph-*GIT3-2* RNAi expression plasmid

The transformation step was performed according to the protocols described by Yu *et al.* (2014) with modifications. A total of 5 µg of the pUChph-*GIT3* RNAi DNA plasmid vector was carefully mixed into 20 µL of PTC buffer (60% PEG 4000, 10 mM Tris-HCl buffer; pH 7.5, 50 mM CaCl₂) before being transferred into the 50 mL Falcon tube containing 100 µL of 1×10^7 protoplasts/mL (protoplasts were suspended in STC solution) respectively. The mixture was incubated at room temperature for 20 min. Then, 10 mL of YMS regeneration broth (0.6 M sucrose, 1.2% glucose, 0.4% g/L peptone, 0.4% yeast extract, and 0.8% malt extract) were added into the mixture and incubated for 10 min at room temperature. Subsequently, warm 10 mL of YMS regeneration agar (0.6 M sucrose, 1.2% glucose, 0.4% g/L peptone, 0.4% yeast extract, 0.8% malt extract and 4% bacteriological agar), were added and the mixture was gently rotated until homogenous and poured onto Petri dishes. The plate was incubated for 2 days at 28°C before being overlaid with PDA containing 20 µg of hygromycin (Calbiochem, USA). The plates were then wrapped with aluminum foil and incubated again at 28°C for 7 to 10 days. Untransformed protoplasts were also treated similarly to the transformed protoplasts and were used as the negative control.

Validation of the putative mutants

The putative mutants that grew on the regeneration media containing 20 µg of hygromycin were sub-cultured onto new PDA plates containing the same concentration of hygromycin and incubated at 28°C for 6 days. This step was repeated twice to obtain putative mutants that stably exhibit the trait of interest for at least up to three generations. Validation of the putative mutants carrying the integrated pUChph-*GIT3* RNAi expression vector was done via the PCR approach using the primers listed in Table 1. All PCR products were sequenced using Sanger sequencing protocols by Apical Scientific Sdn. Bhd. (Malaysia). The genomic DNA extraction was performed using the modified CTAB method (Tamari *et al.*, 2013).

Real-time PCR analysis of gene expression

Quantitative real-time PCR was used to evaluate the levels of *git3* expressed by the wild-type strain (wt) and the RNAi transformants. By filtering the culture medium, 50 mg of mycelia were removed and immediately frozen in liquid nitrogen. The NucleoZOL RNA isolation kit (Macherey-Nagel, Germany) was used to extract total RNA, which was then reverse-transcribed into cDNA using an oligo (dT)20VN primer and random hexamer of the HiscriptIII Reverse Transcriptase (Vazyme, China). Then, using ChamQ Universal SYBR (Vazyme, China) on the iQ5 Real-time PCR (BioRAD, USA), the levels of the housekeeping gene encoding for β-tubulin and *git3* transcript were assessed. The list of primer sequences used for qPCR analysis is as in Table 1. PCR reactions were carried out using the ChamQ Universal SYBR qPCR master mix (Vazyme, China). Following a 30-sec initial denaturation step at 95°C, amplification was carried out in three stages throughout 40 cycles: 15 sec of denaturation at 95°C, 60 sec of annealing at 60°C, and 15 sec of extension at 95°C. For each target, the same PCR conditions were applied. Using the standard curve method, transcript levels were calculated and normalized using the internal control gene for *G. boninense*, the β-tubulin gene. All other transformants were compared to the wild-type mycelia, which served as the reference sample. Expression in the reference sample was set at 1.0, and all other transformants' expression of the *git3* genes is reported as the fold increase or decrease over the reference sample. Relative gene expression levels were calculated after qRT-PCR using the $2^{-\Delta\Delta CT}$ method as described by Livak and Schmittgen (2001).

Pathogenicity test on oil palm plantlet

Three-month-old oil palm plantlets were obtained from MPOB. The *G. boninense* PER71 $\Delta git3$ mutant was cultured on CYM agar plates at 28°C for 5 days. Mycelial plugs with a diameter of 0.8 cm were cut from the culture and used to inoculate sterile test tubes containing the oil palm plantlets. The inoculated plantlets were incubated at room temperature under alternating light and dark conditions. At 10, 20, 30, 60, and 90 days post-inoculation, the infected plantlets were harvested. The basal stem of each plantlet was cut open, stained with lactophenol cotton blue, and examined for morphological

changes. The infected oil palm plantlets were rated based on disease symptoms using a scale ranging from 0 to 5, as described by Goh *et al.* (2016) and shown in Table 2.

Table 1. Oligonucleotide primers for PCR amplifications

Primer	Sequence (5' – 3')	Amplicon size	Description
GIT3-2 F	ACCGTAAAGCTTCTGACGTCCGTCTCCCTCTCTTCTT	2000 kb	Primers for full-length GIT3-2 ORF
GIT3-2 R	TACAGTTCTAGAGTGCAACGCGCTCGTGATATCAGC		
Hygb F	ATGAAAAAGCCTGAACTCAC	1 kb	Primers for full-length hygromycin gene
Hygb R	ATAGTAACCATGGTTGCCTAGTG		
Sense spacer F	AACGAGTGGGGCTAC	591 bp	Primers for sense spacer fragment
Sense spacer R	GAGAGCGGCATGTTTATGAC		
Antisense F	GTCATAAACATGCCGCTCTC	596 bp	Primers for antisense fragment
Antisense R	CCGATGCAAAAATGAGG		
β -tubulin F	GAGTTCACTGAGGCCGAGTC	130 bp	RT-qPCR primer for <i>G. boninense</i> β -tubulin gene (housekeeping)
β -tubulin R	TGCAACACGCTTATTCTTCG		
Git3-2 F	GCATGCTGTTGTATCCGGTG	153 kb	RT-qPCR primer for <i>G. boninense git3</i>
Git3-2 R	GTTGACGACGCCCTGTAAGT		

Table 2. Disease symptom scale

Disease symptom [#]	Scale
Healthy plants with green leaves, absence of fungal mycelium on any part of plants	0
Healthy plants with yellow-green leaves, absence of fungal mycelium on any part of plants	1
Unhealthy plants with chlorotic leaves, absence of fungal mycelium on any part of plants	2
Unhealthy plants with two or three chlorotic leaves, presence of fungal mycelium on basal stem region	3
Unhealthy plants with four or more chlorotic leaves, presence of fungal mycelium on basal stem region	4
Plant death	5

Disease severity was assessed and calculated using the formula by Liu *et al.* (1995) as follows.

$$DSI \% = \frac{\sum (\text{class frequency} \times \text{score of rating class})}{\text{total number of plant} \times \text{maximal disease index}} \times 100$$

RESULTS AND DISCUSSION

Identification and characterization of GPCRs Class III in *G. boninense* PER71

A comprehensive genome search of *G. boninense* G3 and *G. boninense* NJ3, along with a transcriptome analysis of *G. boninense* PER71, was performed to identify genes encoding G protein-coupled receptors (GPCRs). The identified GPCRs were categorized based on homology and structural similarity. This characterization revealed six distinct classes of GPCRs in *G. boninense*: Class II pheromone detectors, Class III carbon sensors, Class IV nitrogen detectors, Class VII proteins such as glycosyltransferases, Class VIII hemolysins, and Class X sensor proteins. The total number of GPCRs identified in each database is summarized in Table 3. Specifically, a total of 16, 23, and 17 GPCRs were identified from the NJ3 genome, G3 genome, and PER71 transcriptome, respectively. Notably, the highest number of GPCRs belonged to Class II, which includes pheromone receptors that play a crucial role in fungal mating.

Studies on other fungi have also identified extensive gene families encoding seven-transmembrane GPCR proteins. In *Aspergillus nidulans*, ten classes of GPCRs, ranging from Class I to Class X, have been identified, including GPCRs that resemble yeast pheromone receptors, the glucose-sensing receptor Gpr1, the nitrogen-starvation sensor Stm1, and cAMP receptors (Han *et al.*, 2004). In *Cryptococcus neoformans*, GPCRs are classified into four groups: rhodopsin, adhesion, glutamate, and frizzled, while in the *Neurospora crassa* genome, ten GPCR proteins have been predicted (Galagan *et al.*, 2003; Xue *et al.*, 2006; Krishnan *et al.*, 2012).

The next step involves characterizing a gene encoding a Class III GPCR from *G. boninense* PER71. A specific member of this group designated Git3, has been selected for further analysis. PCR amplification of the *git3* gene yielded a 1254 bp fragment encoding a protein of 418 amino acids. This

gene is intronless and shows 41% sequence identity to GprD from *Aspergillus nidulans* and 40.71% identity to Gpa2 from *Rhizoctonia solani* at the amino acid level. Figure 1 illustrates a phylogenetic tree constructed using the Maximum Likelihood method with 1000 bootstrap replicates, comparing *G. boninense* Git3 with Class III GPCRs from other fungal species. The analysis reveals that *G. boninense* Git3 is closely related to GprH from *Aspergillus nidulans* and clusters with GprC, GprD, and GprE from the same species, as well as Git3 from *Penicillium expansum* and *A. fumigatus*.

Table 3. Class of GPCRs found in *G. boninense* database

Class of GPCR	NJ3 genome [#]	G3 genome	PER71 transcriptome
Class II	9	10	9
Class III	1	3	2
Class IV	1	0	1
Class VII	3	4	0
Class VIII	0	2	2
Class IX	2	4	2

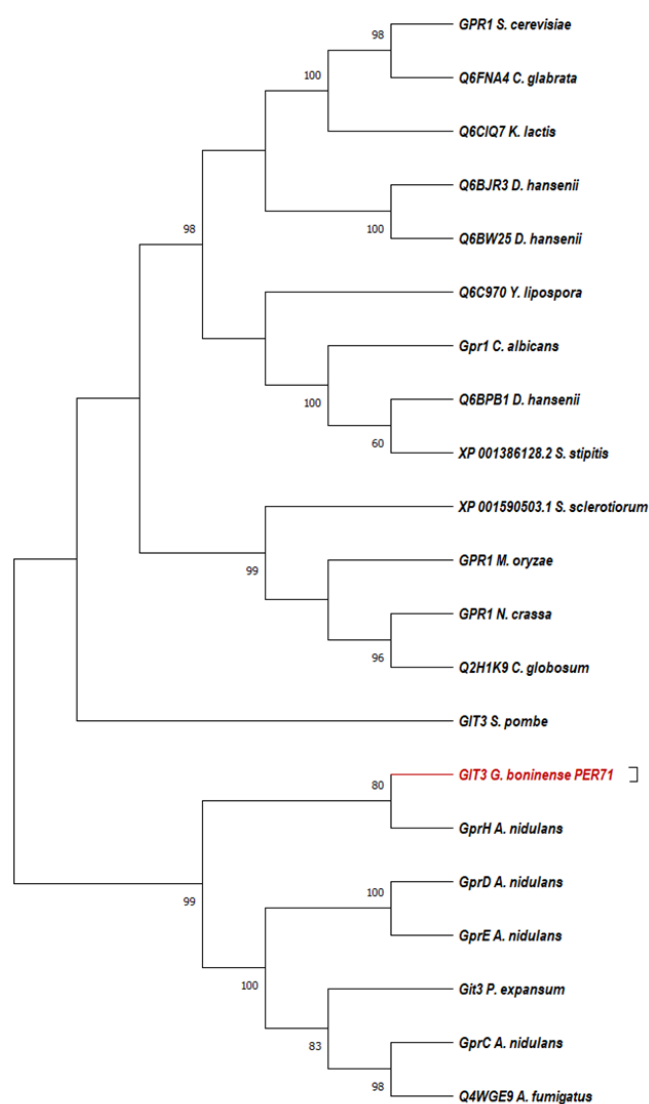


Fig. 1. Phylogenetic tree of *G. boninense* PER71 Git3 compared to Class III GPCRs from various fungi, constructed using the Maximum Likelihood method with 1000 bootstrap replicates. Members of class III used in the tree include sequences from *Schizosaccharomyces pombe* (*S. pombe*), *Penicillium expansum* (*P. expansum*), *Neuspora crassa* (*N. crassa*), *Debaryomyces hansenii* (*D. hansenii*), *Yarrowia lipospora* (*Y. lipospora*), *Candida albican* (*C. albican*), *Aspergillus nidulans* (*A. nidulans*), *Aspergillus fumigatus* (*A. fumigatus*), *Chaetomium globosum* (*C. globosum*), *Magnaporthe oryzae* (*M. oryzae*), *Kluyveromyces lactis* (*K. lactis*), *Sclerotinia sclerotiorum* (*S. sclerotiorum*) and *Candida glabrata* (*C. glabrata*). *G. boninense* is highlighted in red.

Subsequently, a multiple sequence alignment using TCOFFEE Transmembrane MSA was conducted

to identify conserved domains between Git3 of *G. boninense* PER71 and other known glucose sensors in *Schizosaccharomyces pombe*, *P. expansum*, *N. crassa*, *Debaryomyces hansenii*, *Yarrowia lipolytica*, *Candida albicans*, *A. nidulans*, *A. fumigatus*, *Chaetomium globosum*, *M. oryzae*, *Cluyveromyces lactis*, *Sclerotinia sclerotiorum*, *Candida glabrata*, *Spathaspora passalidarum*, and *Arabidopsis thaliana*. Figure 2(a) highlights a conserved region in the extracellular loop with a specific amino acid marked by an asterisk at position 179. This suggests that this region might be an important binding site for the receptor protein; however, the function of this region has not been studied. Figure 2(b) shows that the Git3 protein consists of seven transmembrane domains with three extracellular loops and an extended intracellular tail, visualized using Protter (<https://wlab.ethz.ch/protter/start/>). In *A. nidulans*, an extended loop is also found in the third cytoplasmic loop and tail (Brown et al., 2018).

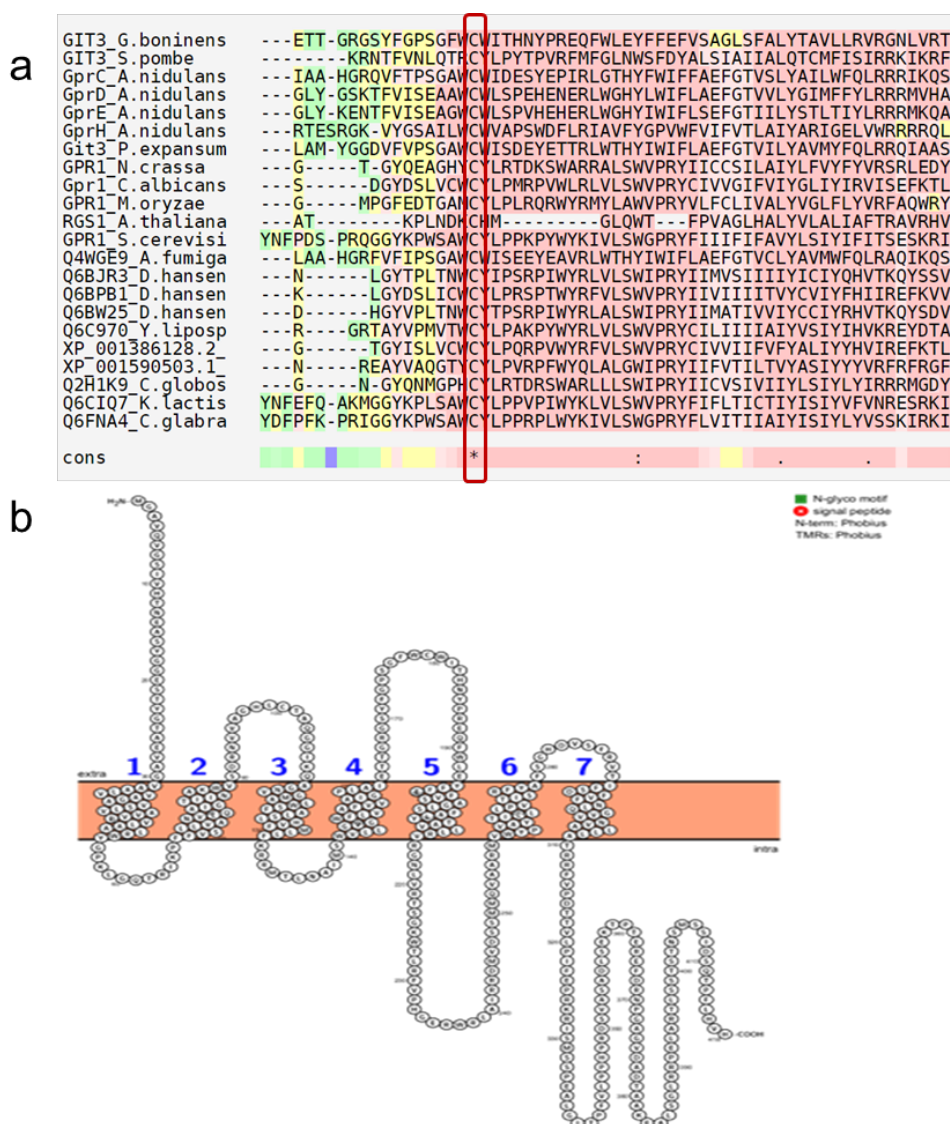


Fig. 2. (a) Multiple sequence alignment using TCOFFEE of Git3 *G. boninense* PER71 with glucose sensors of other fungi including *S. pombe*, *P. expansum*, *N. crassa*, *D. hansenii*, *Y. lipospora*, *C. albican*, *A. nidulans*, *A. fumigatus*, *C. globosum*, *M. oryzae*, *K. lactis*, *S. sclerotiorum*, *C. glabrata*, *S. stipites* and *A. thaliana*. Red colored shows a highly conserved region (b) Visualisation of Git3 protein by Protter software demonstrating the presence of seven transmembrane regions.

Development of vectors containing siRNA expression cassettes and quantification of *git3* expression in *G. boninense* transformants using real-time qPCR

The pUChph-Git3 plasmid was designed to encode a hairpin RNA consisting of two complementary 511 bp regions of the *git3* gene, separated by an 80 bp spacer. The silencing plasmid was introduced into *G. boninense* through PEG-mediated transformation. All transformants were cultured on a PDA medium containing 20 µg/mL hygromycin. Five stable transformants were obtained after three generations of growth on the selective medium and were selected for further analysis. The *git3*-silenced mutants were

able to grow on a medium containing the hygromycin, whereas non-silenced transformants could not. Figure 3 shows the presence of the hygromycin resistance gene (*hph*) in the five selected mutants, as confirmed by PCR using Hygb primers, corroborating the observed growth on hygromycin-selective media. PCR amplification using the sense, spacer, and antisense primers also detected the presence of the full-length RNAi cassette in the mutants. This suggests that the silencing cassette has been successfully integrated into the *G. boninense* genome.

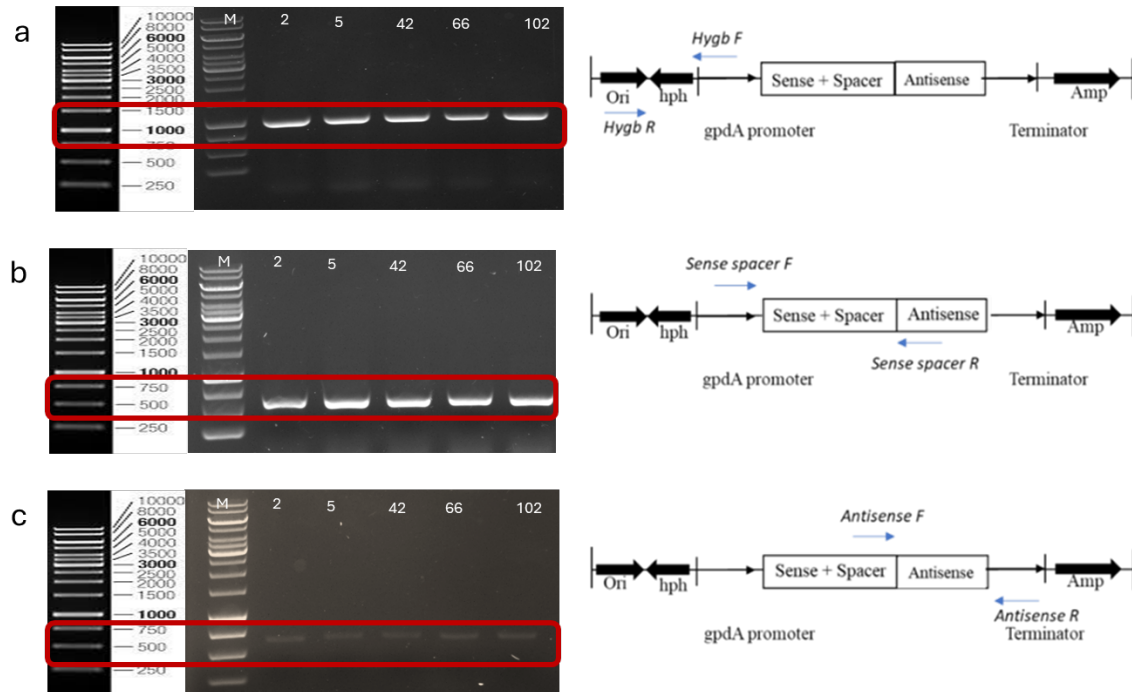


Fig. 3. PCR products of the $\Delta git3$ mutants (a) PCR product of $\Delta git3$ mutant using hygromycin primer with the expected size of 1 kb (b) PCR product of $\Delta git3$ mutant with Sense-spacer primer with the expected size of 591 bp (c) PCR product of $\Delta git3$ mutant using antisense primer with the expected product of 596 bp.

Real-time qPCR was employed to analyze the RNAi-mediated pUChph-GIT3 transformants at the molecular level. The transcription levels of the β -tubulin gene were used to normalize the *git3* expression levels. To determine the reduction in mRNA transcript levels at the *git3* locus, five positive transformants were selected for real-time qPCR analysis. Three of the five transformants showed a reduction in *git3* gene expression, albeit to varying degrees. Figure 4 illustrates the relative gene expression of *git3* compared to the wild-type *G. boninense* PER71, with mutant 42 exhibiting the highest reduction, significantly suppressing *git3* expression by 47%. Mutants 66 and 5 also showed reductions in comparison to the wild type, but at lower levels of 23% and 13%, respectively. Previous studies in *Candida glabrata* and *Ganoderma lucidum* have reported that shRNA caused a reduction in transcription by approximately 50% to 60% (Mu *et al.*, 2012; Ishchuk *et al.*, 2019). However, for the remaining mutants, no significant reduction in *git3* expression was observed. This lack of significant reduction may be attributed to factors such as gene mistargeting in the RNAi system, sequence homology, incomplete repression, seed region complementarity to unintended target genes, secondary structure of the target mRNA, and the delivery method, which have been reported to cause non-specific effects on gene expression (McIntyre & Fanning, 2006).

Pathogenicity test on oil palm plantlet and Disease Severity Index of *G. boninense* transformants

The pathogenicity test conducted on oil palm plantlets showed that those inoculated with the $\Delta git3$ mutant did not exhibit any reduction in disease. Conversely, the control, uninfected plantlets displayed no disease symptoms after 90 days. As shown in Figure 5, symptoms of infection began to appear in all infected plantlets at the basal stem after 30 days of infection. The basal stem turned yellow, wet, very soft, and mushy, unlike the uninfected plantlets, which only showed a yellow color but maintained a rigid basal stem. The upper stems and leaves of all tested plantlets did not display any disease symptoms at this stage. It was only after 60 days of infection that the leaves started to show chlorotic symptoms, except in the control uninfected plantlets. After 90 days, all infected plantlets, whether with the wild-type

G. boninense PER71 or the $\Delta git3$ mutant, had dry and brittle basal stems, with most leaves wilting. Dikaryotic mycelia were successfully re-isolated from the symptomatic infected tissues, as shown in Figure 6. In *A. fumigatus*, deletion of corresponding genes resulted in drastic growth defects, including reduced hyphal extension, retarded germination, and elevated levels of branching. However, in *G. boninense* PER71, the knockdown of *git3* did not cause any of these effects, as shown in Figure 6.

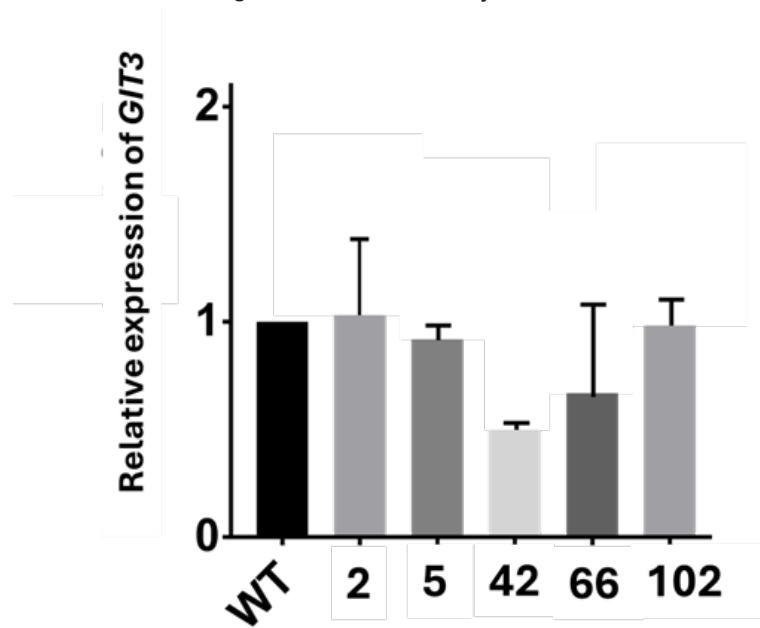


Fig. 4. Gene expression of *git3* in the wild-type and $\Delta git3$ mutants using real-time qPCR

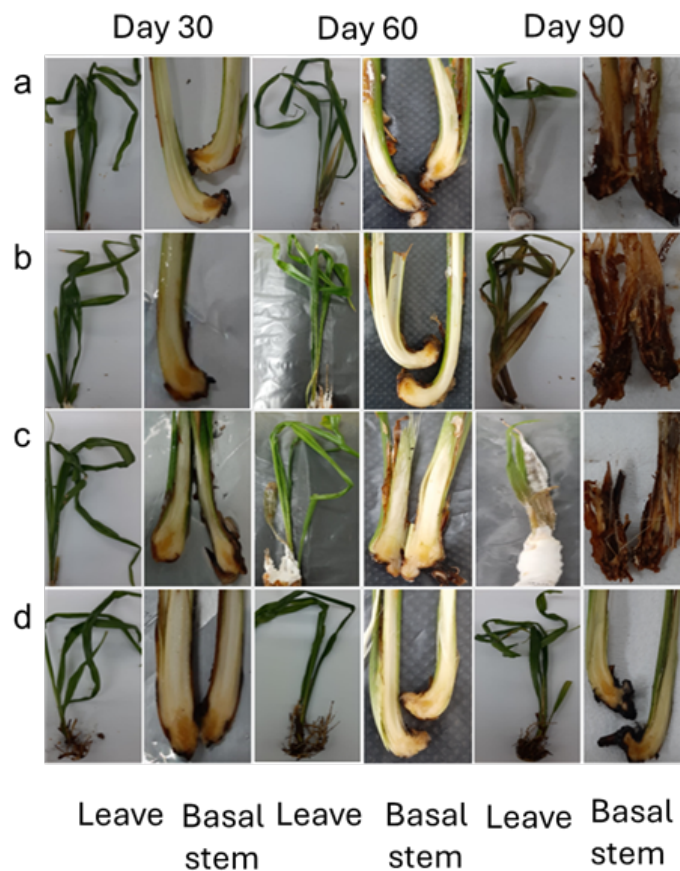


Fig. 5. Infected oil palm plantlet after 30 days, 60 days, and 90 days infection. (a) oil palm infected with Mutant 42. (b) oil palm plantlet infected with Mutant 66 (c) oil palm plantlet infected with wild-type *G. boninense* PER71 (d) uninfected oil palm plantlet.

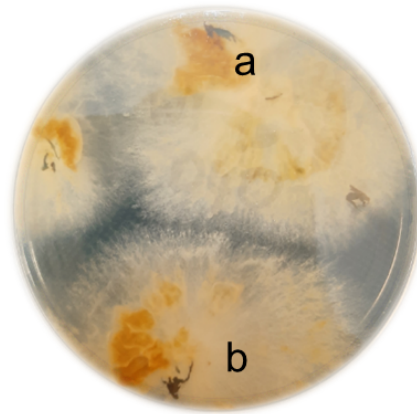


Fig. 6. Re-isolated dikaryotic mycelia from infected basal stem tissues from (a) Mutant 42 and (b) Mutant 66.

The disease severity among isolates varied between 80-100%. As it was difficult to visually assess the severity in infected oil palm plantlets, a one-way ANOVA test was used to analyze the significant differences between treatments. The one-way ANOVA test indicated a significant difference ($p < 0.05$) between oil palm plantlets infected with wild-type *G. boninense* PER71 and those infected with the *git3* mutant. Mutant 42 exhibited the lowest disease severity index, with 40% severity at day 80, while mutant 66 showed 70% severity, compared to 80% in the wild-type at the same time point. By day 90, all infected plantlets, whether with the wild-type or *git3* mutants, were completely dead. This result suggests that *Git3* might play a role during the early stages of infection, as the mutants were able to slow down the progression of infection, as demonstrated by the DSI. However, after 90 days, the mutants exhibited a similar pattern of lethality to the wild-type, indicating that while *Git3* may be involved in the early stages of infection, once the fungus enters the plant, other pathogenicity factors take over, leading to the plant's eventual death.

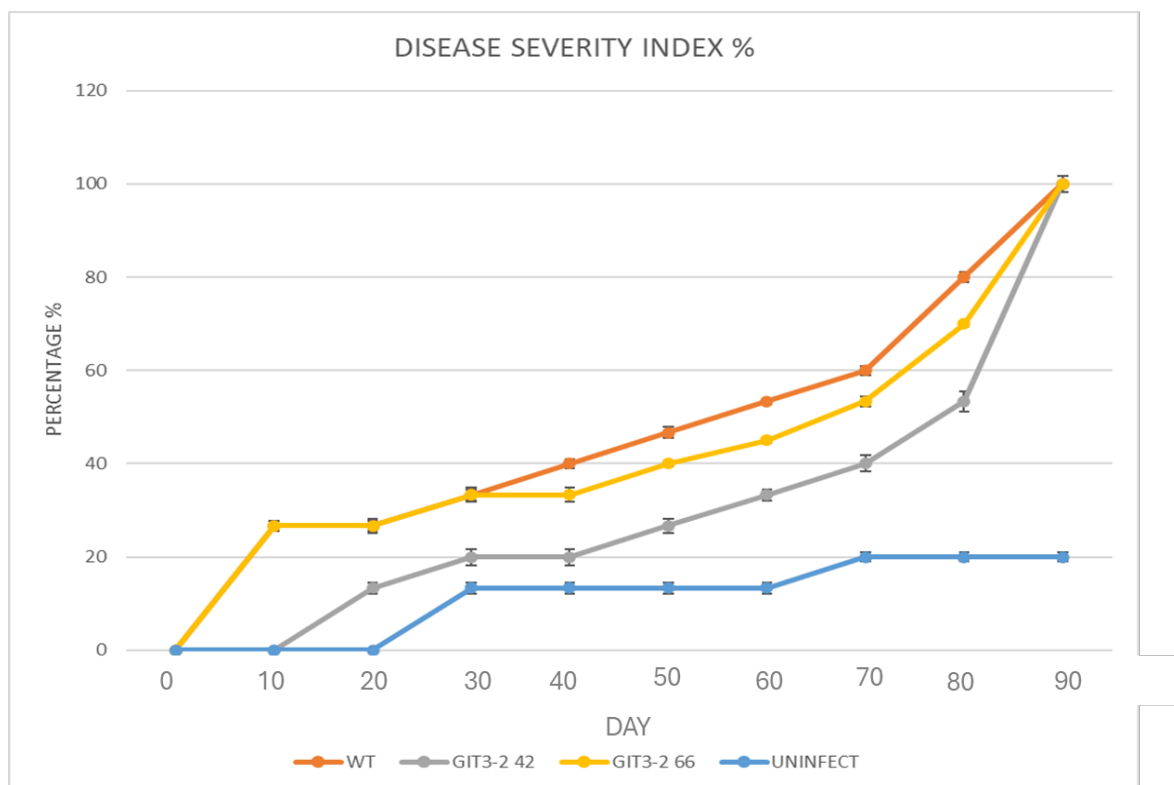


Fig. 7. Disease Severity Index (DSI) of oil palm plantlets infected with $\Delta git3$ mutants (mutant 42 and 66), wild-type (WT), and control oil palm (uninfected) for 90 days.

CONCLUSION

In this study, we identified six classes of G protein-coupled receptors (GPCRs) in *G. boninense* and successfully developed a shRNA interference system targeting *git3* in *G. boninense* PER71. Although the number of mutants generated was relatively low, the observed reduction in gene expression among the *git3* mutants was comparable to findings from previous RNAi studies in other *Ganoderma* species. Pathogenicity tests on oil palm plantlets indicated that *Git3* may play a role during the early stages of *G. boninense* infection, as the mutants were able to slow the progression of infection in oil palm plantlets. Future research should aim to increase the number of mutants produced through the shRNA interference system to further elucidate the functional roles of *Git3* and other GPCRs in *G. boninense*.

ACKNOWLEDGEMENTS

This work was supported by the Ministry of Higher Education (MoHE), Malaysia under the Grant FRGS/1/2019/STG03/UKM/02/2.

ETHICAL STATEMENT

Not applicable

CONFLICT OF INTEREST

The authors declare no conflict of interest.

REFERENCES

- Affeldt, K.J., Brodhagen, M. & Keller, N.P. 2012. Aspergillus oxylipin signaling and quorum sensing pathways depend on G protein-coupled receptors. *Toxins*, 4(9): 695-717. <https://doi.org/10.3390/toxins4090695>
- Azmi, A.N.N., Bejo, S.K., Jahari, M., Muharam, F.M., Yule, I. & Husin, N.A. 2020. Early detection of *Ganoderma boninense* in oil palm seedlings using support vector machines. *Remote Sensing*, 12(23): 1-21. <https://doi.org/10.3390/rs12233920>
- Bharudin, I., Ab Wahab, A.F.F., Abd Samad, M.A., Xin Yie, N., Zairun, M.A., Abu Bakar, F.D. & Murad, A.M.A. 2022. Review update on the life cycle, plant-microbe interaction, genomics, detection and control strategies of the oil palm pathogen *Ganoderma boninense*. *Biology*, 11(2): 1-18. <https://doi.org/10.3390/biology11020251>
- Brown, N.A., Schrevens, S., Van Dijck, P. & Goldman, G. H. 2018. Fungal G-protein-coupled receptors: Mediators of pathogenesis and targets for disease control. *Nature Microbiology*, 3(4): 402-414. <https://doi.org/10.1038/s41564-018-0127-5>
- El-Defrawy, M.M.H. & Hesham, A.E.L. 2020. G-protein-coupled receptors in fungi. In: *Fungal Biotechnology and Bioengineering*. A.E. Hesham, R.S. Upadhyay, G.D.Sharma, C. Manoharachary and V.K. Gupta (Eds.). Springer Nature, Switzerland. 37-126 pp. https://doi.org/10.1007/978-3-030-41870-0_3
- Galagan, J.E., Calvo, S.E., Borkovich, K.A., Selker, E.U., Read, N.O., Jaffe, D., FitzHugh, W., Ma, L.J., Smirnov, S., Purcell, S., Rehman, B., Elkins, T., Engels, R., Wang, S., Nielsen, C.B., Butler, J., Endrizzi, M., Qui, D., Ianakiev, P. & Birren, B. 2003. The genome sequence of the filamentous fungus *Neurospora crassa*. *Nature*, 422(6934): 859-868. <https://doi.org/10.1038/nature01554>
- Gao, J., Xu, X., Huang, K. & Liang, Z. 2021. Fungal G-protein-coupled receptors: A promising mediator of the impact of extracellular signals on biosynthesis of ochratoxin A. *Frontiers in Microbiology*, 12(February): 1-15. <https://doi.org/10.3389/fmicb.2021.631392>
- Gehrke, A., Heinekamp, T., Jacobsen, I.D. & Brakhage, A.A. 2010. Heptahelical receptors GprC and GprD of *Aspergillus fumigatus* are essential regulators of colony growth, hyphal morphogenesis, and virulence. *Applied and Environmental Microbiology*, 76(12): 3989-3998. <https://doi.org/10.1128/AEM.00052-10>
- Goh, K.M., Dickinson, M., Alderson, P., Yap, L.V. & Supramaniam, C.V. 2016. Development of an in planta infection system for the early detection of *Ganoderma* spp. in oil palm. *Journal of Plant Pathology*, 98(2): 255-264.
- Han, K.H., Seo, J.A. & Yu, J.H. 2004. A putative G protein-coupled receptor negatively controls sexual development in *Aspergillus nidulans*. *Molecular Microbiology*, 51(5): 1333-1345. <https://doi.org/10.1111/j.1365-2958.2003.03940.x>
- Hofmann, K. & Stoffel, W. 1993. Tmbase-A database of membrane spanning protein segments [WWW Document]. URL <https://api.semanticscholar.org/CorpusID:83288447> (accessed 8.22.23).
- Isaac, I.L., Walter, A.W.C.Y., Bakar, M.F.A., Idris, A.S., Bakar, F.D.A., Bharudin, I. & Murad, A.M.A. 2018. Transcriptome datasets of oil palm pathogen *Ganoderma boninense*. *Data in Brief*, 17: 1108-1111. <https://doi.org/10.1016/j.dib.2018.02.027>
- Ishchuk, O.P., Ahmad, K.M., Koruza, K., Bojanovič, K., Sprenger, M., Kasper, L., Brunke, S., Hube, B.,

- Säll, T., Hellmark, T., Gullstrand, B., Brion, C., Freil, K., Schacherer, J., Regenber, B., Knecht, W. & Piškur, J. 2019. RNAi as a tool to study virulence in the pathogenic yeast *Candida glabrata*. *Frontiers in Microbiology*, 10: 1679. <https://doi.org/10.3389/fmicb.2019.01679>
- Käll, L., Krogh, A. & Sonnhammer, E.L.L. 2007. Advantages of combined transmembrane topology and signal peptide prediction-the Phobius web server. *Nucleic Acids Research*, 35(SUPPL.2): 429-432. <https://doi.org/10.1093/nar/gkm256>
- Khairi, M.H.F., Nor Muhammad, N.A., Bunawan, H., Murad, A.M.A. & Ramzi, A.B. 2022. Unveiling the core effector proteins of oil palm pathogen *Ganoderma boninense* via pan-secretome analysis. *Journal of Fungi*, 8(8): 793. <https://doi.org/10.3390/jof8080793>
- Khaled, A.Y., Abd Aziz, S., Khairunniza Bejo, S., Mat Nawi, N., Jamaludin, D. & Ibrahim, N.U.A. 2020. A comparative study on dimensionality reduction of dielectric spectral data for the classification of basal stem rot (BSR) disease in oil palm. *Computers and Electronics in Agriculture*, 170(Febuary): 105288. <https://doi.org/10.1016/j.compag.2020.105288>
- Kraakman, L., Lemaire, K., Ma, P., Teunissen, W., Donaton, M.C., Van Dijck, P., Winderickx, J., de Winde, J.H. & Thevelein, J.M. 1999. A *Saccharomyces cerevisiae* G-protein coupled receptor, Gpr1, is specifically required for glucose activation of the cAMP pathway during the transition to growth on glucose. *Molecular Microbiology*, 32(5): 1002-1012. <https://doi.org/10.1046/j.1365-2958.1999.01413.x>
- Krishnan, A., Almén, M.S., Fredriksson, R. & Schiöth, H.B. 2012. The origin of GPCRs: Identification of mammalian like rhodopsin, adhesion, glutamate and frizzled GPCRs in fungi. *PLoS ONE*, 7(1): 29817. <https://doi.org/10.1371/journal.pone.0029817>
- Lafon, A., Han, K.H., Seo, J.A., Yu, J.H. & d'Enfert, C. 2006. G-protein and cAMP-mediated signaling in aspergilli: A genomic perspective. *Fungal Genetics and Biology*, 43(7): 490-502. <https://doi.org/10.1016/j.fgb.2006.02.001>
- Liu, L., Kloepper, J.W. & Tuzun, S. 1995. Induction of systemic resistance in cucumber against bacterial angular leaf spot by plant growth-promoting rhizobacteria. *Phytopathology*, 85: 843-847. <https://doi.org/10.1094/Phyto-85-843>
- Livak, K.J. & Schmittgen, T.D. 2001. Analysis of relative gene expression data using real-time quantitative PCR and the 2- $\Delta\Delta$ CT method. *Methods*, 25(4): 402-408. <https://doi.org/10.1006/meth.2001.1262>
- Madihah, A.Z., Maizatul-Suriza, M., Idris, A.S., Bakar, M.F.A., Kamaruddin, S., Bharudin, I., Abu Bakar, F.D. & Murad, A.M.A. 2018. Comparison of DNA extraction and detection of *Ganoderma*, causal of basal stem rot disease in oil palm using loop-mediated isothermal amplification. *Malaysian Applied Biology*, 47(5): 119-127.
- McIntyre, G.J. & Fanning, G.C. 2006. Design and cloning strategies for constructing shRNA expression vectors. *BMC Biotechnology*, 6: 1-8. <https://doi.org/10.1186/1472-6750-6-1>
- Mercière, M., Laybats, A., Carasco-Lacombe, C., Tan, J.S., Klopp, C., Durand-Gassel, T., Alwee, S.S.R.S., Camus-Kulandaivelu, L. & Breton, F. 2015. Identification and development of new polymorphic microsatellite markers using genome assembly for *Ganoderma boninense*, causal agent of oil palm basal stem rot disease. *Mycological Progress*, 14: 103. <https://doi.org/10.1007/s11557-015-1123-2>
- Mu, D., Shi, L., Ren, A., Li, M., Wu, F., Jiang, A. & Zhao, M. 2012. The development and application of a multiple gene co-silencing system using endogenous URA3 as a reporter gene in *Ganoderma lucidum*. *PLoS ONE*, 7(8): e43737. <https://doi.org/10.1371/journal.pone.0043737>
- Notredame, C., Higgins, D.G. & Heringa, J. 2000. T-coffee: A novel method for fast and accurate multiple sequence alignment. *Journal of Molecular Biology*, 302(1): 205-217. <https://doi.org/10.1006/jmbi.2000.4042>
- Nur-Rashyeda, R., Idris, A.S., Sundram, S., Zainol-Hilmi, N.H. & Ming, S.C. 2023. A field evaluation in fungicides application to control upper stem rot (USR) disease in oil palm caused by *Ganoderma* spp. *Journal of Oil Palm Research*, 35(2): 320-329.
- Paterson, R.R.M. 2019. *Ganoderma boninense* disease of oil palm to significantly reduce production after 2050 in sumatra if projected climate change occurs. *Microorganisms*, 7(1): 4-6. <https://doi.org/10.3390/microorganisms7010024>
- Raudaskoski, M. & Kothe, E. 2010. Basidiomycete mating type genes and pheromone signaling. *Eukaryotic Cell*, 9(6): 847-859. <https://doi.org/10.1128/EC.00319-09>
- Rubio-Teixeira, M., Van Zeebroeck, G., Voordeckers, K. & Thevelein, J.M. 2010. *Saccharomyces cerevisiae* plasma membrane nutrient sensors and their role in PKA signaling. *FEMS Yeast Research*, 10(2): 134-149. <https://doi.org/10.1111/j.1567-1364.2009.00587.x>
- Sonnhammer, E.L., von Heijne, G. & Krogh, A. 1998. A hidden Markov model for predicting transmembrane helices in protein sequences. In: *Proceedings International Conference on Intelligent Systems for Molecular Biology*. ISMB, 6: 175-182.
- Sulaiman, S., Othman, N.Q., Tan, J.S. & Lee, Y.P. 2020. Draft genome assembly dataset of the Basidiomycete pathogenic fungus, *Ganoderma boninense*. *Data in Brief*, 29: 105167. <https://doi.org/10.1016/j.dib.2020.105167>
- Tamari, F., Hinkley, C.S. & Ramprasad, N. 2013. A comparison of DNA extraction methods using

- Petunia hybrida* tissues. Journal of Biomolecular Techniques, 24(3): 113-118.
- Tamura, K., Stecher, G. & Kumar, S. 2021. MEGA11: Molecular Evolutionary Genetics Analysis Version 11. Molecular Biology and Evolution, 38(7): 3022-3027. <https://doi.org/10.1093/molbev/msab120>
- Utomo, C., Tanjung, Z.A., Aditama, R., Buana, R.F.N., Pratomo, A.D.M., Tryono, R. & Liwang, T. 2018. Draft genome sequence of the phytopathogenic fungus *Ganoderma boninense*, the causal agent of basal stem rot disease on oil palm. Genome Announcements, 6(17): e00122-18. <https://doi.org/10.1128/genomeA.00122-18>
- Wess, J., Han, S.J., Kim, S.K., Jacobson, K.A. & Li, J.H. 2008. Conformational changes involved in G-protein-coupled-receptor activation. Trends in Pharmacological Sciences, 29(12): 616-625. <https://doi.org/10.1016/j.tips.2008.08.006>
- Xue, C., Bahn, Y.S., Cox, G.M. & Heitman, J. 2006. G protein-coupled receptor Gpr4 senses amino acids and activates the cAMP-PKA pathway in *Cryptococcus neoformans*. Molecular Biology of the Cell, 17(2): 667-679. <https://doi.org/10.1091/mbc.e05-07-0699>
- Yu, X., Ji, S.L., He, Y.L., Ren, M.F. & Xu, J.W. 2014. Development of an expression plasmid and its use in genetic manipulation of Lingzhi or Reishi Medicinal Mushroom, *Ganoderma lucidum* (Higher Basidiomycetes). International Journal of Medicinal Mushrooms, 16(2): 161-168. <https://doi.org/10.1615/IntJMedMushr.v16.i2.60>

